International Tables for Crystallography (2010). Vol. B, Section 2.5.3.3.6, pp. 334–344.

2.5.3.14(*a*) and (*b*) were taken for FeS_2, space group $P2_1/a\bar{3}$, with incident-beam directions of [100] and [110]. Inserts show enlarged HOLZ patterns for ease of viewing. Extinction lines of type *A* are seen in the h_ok0 HOLZ reflections in Fig. 2.5.3.14(*a*) due to the *b*-glide plane (equivalent to the *a*-glide plane in the space-group symbol) parallel to the (001) plane. An extinction line A^* is seen in an h_ok0 HOLZ reflection in Fig. 2.5.3.14(*b*) due to the same glide plane as that of Fig. 2.5.3.14(*a*). It should be noted that extinction lines in HOLZ reflections are better observed in thinner specimen areas than those suitable for the observation of the extinction lines in ZOLZ reflections, because the profiles of HOLZ reflections are concentrated into small areas of CBED discs in thicker specimens.

In summary, the use of not only ZOLZ, but also HOLZ extinction lines is recommended for space-group determination.

2.5.3.3.5. *Symmetry elements observed by CBED*

In the above sections, point-group and space-group determination methods were described following the theory of Buxton *et al.* (1976). They assumed that the observable symmetry elements are those of an infinitely extended parallel-sided specimen or of diperiodic plane figures. CBED patterns determine diffraction groups. Crystal point groups are identified by consulting Fig. 2.5.3.4, which gives the relations between diffraction groups and crystal point groups. When the assumption made by Buxton *et al.* (1976) is accepted in a strict sense, CBED symmetry m_2 caused by a twofold rotation axis oblique to the specimen surface, which is not a symmetry element of a diperiodic plane figure, ought not to be observed. However, the symmetry m_2 due to a twofold rotation axis in the $[1\bar{1}0]$ direction of an Si film with [100] surface normal has been clearly observed at [111] electron incidence (Tanaka *et al.*, 1988, p. 33). This indicates that crystal symmetry elements oblique to the specimen surface are observable when the specimen is tilted. An important condition for CBED is that the top and bottom surfaces be parallel over the specimen area illuminated by the incident beam. CBED observes the symmetry elements of a crystal to the extent that the boundary conditions at the specimen surface do not break the symmetries of the CBED patterns. Gjønnes & Gjønnes (1985) reported that the breaking of CBED symmetry due to a surface oblique to the incident beam is practically negligible.

In Section 2.5.3.3 on space-group determination, space-group symmetry elements of crystals which have glide and screw components parallel to the specimen surface were considered to act as space-group symmetry elements of diperiodic plane figures by mitigating the strict application of the assumption of diperiodic plane figures. In fact, vertical glide planes with a glide vector not parallel to the specimen surface, which were dealt in Section 2.5.3.3.4, are not the symmetry elements of diperiodic plane figures. Ishizuka (1982) showed theoretically that a vertical glide plane with a vertical glide vector produces dynamical extinction lines in HOLZ discs if the Laue zones are well separated. Tanaka *et al.* (1988, pp. 214–225) tabulated the extinction lines appearing in HOLZ discs caused by the vertical glide planes whose glide vectors are not only parallel but also not parallel to the specimen surface. Dynamical extinction lines caused by the glide planes with a glide vector not parallel to the surface have been demonstrated using FeS_2 and $MgAl_2O_4$ (Tanaka *et al.*, 1988, pp. 51–61).

Vertical 2_1, 3_1, 3_2, ..., 6_5 screw axes, which are not symmetry elements of diperiodic plane figures, are expected to form dynamical extinction lines in kinematically forbidden reflections that are located in the direction of the screw axes or of the surface normal. The extinction lines, however, are difficult to observe in ordinary CBED. Thus, CBED does not observe all the symmetry elements of the crystal space groups but observes many more symmetry elements than those of the diperiodic plane figures. It is clear now that it makes no sense to construct space groups using actually observable symmetry elements because they do not form a complete set of groups. It is of no importance to give the relation between the 230 space groups of crystals and the 80 space groups of diperiodic plane figures. Buxton *et al.*'s theory, which determines crystal point groups with the help of diperiodic plane figures, is very beautiful and successful. However, it is not correct to state that CBED observes the symmetry elements of the diperiodic plane figures. The use of the groups of diperiodic plane figures should be recognized as a convention for the sake of convenience. As a further example, horizontal screw axes and horizontal glide planes must be located at the middle of a specimen to form symmetry elements of the diperiodic plane figures. However, those screw axes and glide planes which are not located at the middle of a specimen do produce CBED symmetries. Since we now know that CBED does not observe the symmetries of the diperiodic plane figures but observes those of a physical crystalline specimen, we can determine the corresponding infinite crystal symmetries more freely, by using our knowledge of the symmetries of the sample concerned, guided but not restricted by the beautiful theory of Buxton *et al.* (1976).

One point to note, for symmetry determination, is that one has to be aware of spurious symmetries that appear for crystals of certain structure types (Tanaka *et al.*, 1988, pp. 20–32 and 42–45) and destroy the correct determination of the point and space groups. Another point for precise symmetry determination is that one has to be aware of how CBED symmetry is destroyed by a small breakdown of crystal symmetry (Tanaka *et al.*, 1988 pp. 46–47).

2.5.3.3.6. *Examples of space-group determination*

A simple example of point-group determination has already been given for Si in Section 2.5.3.2.5. In this section, two examples of space-group determination for rutile and samarium selenide are described, in which the point-group determination still accounts for an important part. The examples look to be a little sophisticated but are a good exercise for those who want to acquire experience in CBED space-group determination. The present determination is carried out by assuming the lattice parameters to be known.

Rutile (TiO_2). The space group of rutile is well known to be $P4_2/mnm$. The lattice parameters are $a = b = 0.459$ nm and $c = 0.296$ nm. Fig. 2.5.3.15(*a*) shows a CBED pattern taken with the [001] incidence at an accelerating voltage of 80 kV. Since no fine HOLZ lines appear in all the discs, projection diffraction groups (column VI of Table 2.5.3.3) have to be applied to explain this pattern. The projection (proj.) WP shows symmetry $4mm$. The projection diffraction group is found to be $4mm1_R$ from Table 2.5.3.3. Thus, possible diffraction groups are $4m_Rm_R$, $4mm$, 4_Rmm_R and $4mm1_R$. Another CBED pattern at a second crystal orientation needs to be taken because Fig. 2.5.3.15(*a*) shows only projection symmetry. Figs. 2.5.3.15(*b*) and (*c*) show CBED patterns taken with the [101] incidence at an accelerating voltage of 100 kV. In Fig. 2.5.3.15(*b*), which is the central part of Fig. 2.5.3.15(*c*), no HOLZ lines are seen. The symmetries of the projection BP and projection WP are both $2mm$. The projection diffraction group of the pattern is $2mm1_R$. The WP of Fig. 2.5.3.15(*c*) is seen to have one mirror symmetry *m*. The diffraction groups which satisfy symmetry *m* are *m*, $m1_R$ and 2_Rmm_R. Among these diffraction groups, the diffraction group whose projection becomes $2mm1_R$ is only diffraction group 2_Rmm_R. By consulting Fig. 2.5.3.4, diffraction group 2_Rmm_R obtained from Figs. 2.5.3.15(*b*) and (*c*) and one diffraction group $4mm1_R$ among diffraction groups $4m_Rm_R$, $4mm$, 4_Rmm_R and $4mm1_R$ obtained from Fig. 2.5.3.15(*a*) commonly satisfy point group $4/mmm$. Thus, the point group of rutile is determined to be $4/mmm$.

Fig. 2.5.3.15(*d*) shows an ordinary diffraction pattern taken with the [001] incidence at an accelerating voltage of 80 kV. With the help of the lattice parameters and the camera length, the indices of the reflections are given as shown in the figure. There

Table 2.5.3.12. *Dynamical extinction lines appearing in HOLZ reflections for crystal space groups that have mirror and glide planes*

Point groups m, $2/m$ (second setting, unique axis b)

Space group		Incident-beam direction	
		$[u0w]$	
6	Pm		
7	Pc	$h0l_o$ c	A_h
8	Cm		
9	Cc	h_e0l_o c	A_h
10	$P2/m$		
11	$P2_1/m$		
12	$C2/m$		
13	$P2/c$	$h0l_o$ c	A_h
14	$P2_1/c$	$h0l_o$ c	A_h
15	$C2/c$	h_e0l_o c	A_h

Point group $mm2$

Space group		Incident-beam direction									
		[100]		[010]		[001]		$[0vw]$		$[u0w]$	
25	$Pmm2$										
26	$Pmc2_1$	$h0l_o$ c	A			$h0l_o$ c	A			$h0l_o$ c	A_h
27	$Pcc2$	$h0l_o$ c_2	A	$0kl_o$ c_1	A	$0kl_o$ c_1 $h0l_o$ c_2	A	$0kl_o$ c_1	A_h	$h0l_o$ c_2	A_h
28	$Pma2$	h_o0l a	A			h_o0l a	A			h_o0l a	A_h
29	$Pca2_1$	h_o0l a	A	$0kl_o$ c	A	$0kl_o$ c h_o0l a	A	$0kl_o$ c	A_h	h_o0l a	A_h
30	$Pnc2$	$h0l_o$ c	A	$0kl$: $k + l = 2n + 1$ n	A	$0kl$: $k + l = 2n + 1$ n $h0l_o$ c	A	$0kl$: $k + l = 2n + 1$ n	A_h	$h0l_o$ c	A_h
31	$Pmn2_1$	$h0l$: $h + l = 2n + 1$ n	A			$h0l$: $h + l = 2n + 1$ n	A			$h0l$: $h + l = 2n + 1$ n	A_h
32	$Pba2$	h_o0l a	A	$0k_ol$ b	A	$0k_ol$ b h_o0l a	A	$0k_ol$ b	A_h	h_o0l a	A_h
33	$Pna2_1$	h_o0l a	A	$0kl$: $k + l = 2n + 1$ n	A	$0kl$: $k + l = 2n + 1$ n h_o0l a	A	$0kl$: $k + l = 2n + 1$ n	A_h	h_o0l a	A_h
34	$Pnn2$	$h0l$: $h + l = 2n + 1$ n_2	A	$0kl$: $k + l = 2n + 1$ n_1	A	$0kl$: $k + l = 2n + 1$ n_1 $h0l$: $h + l = 2n + 1$ n_2	A	$0kl$: $k + l = 2n + 1$ n_1	A_h	$h0l$: $h + l = 2n + 1$ n_2	A_h
35	$Cmm2$ $ba2$										
36	$Cmc2_1$ $bn2_1$	h_e0l_o c	A			h_e0l_o c	A			h_e0l_o c	A_h
37	$Ccc2$ $nn2$	h_e0l_o c_2	A	$0k_el_o$ c_1	A	$0k_el_o$ c_1 h_e0l_o c_2	A	$0k_el_o$ c_1	A_h	h_e0l_o c_2	A_h

Table 2.5.3.12 (*cont.*)

Space group	Incident-beam direction									
	[100]		[010]		[001]		[0*vw*]		[*u*0*w*]	
38 *Amm*2 *nc*2_1										
39 *Abm*2 *cc*2_1			$0k_ol_o$ *b*	*A*	$0k_ol_o$ *b*	*A*	$0k_ol_o$ *b*	A_h		
40 *Ama*2 *nn*2_1	h_o0l_e *a*	*A*			h_o0l_e *a*	*A*			h_o0l_e *a*	A_h
41 *Aba*2 *cn*2_1	h_o0l_e *a*	*A*	$0k_ol_o$ *b*	*A*	$0k_ol_o$ *b* h_o0l_e *a*	*A*	$0k_ol_o$ *b*	A_h	h_o0l_e *a*	A_h
42 *Fmm*2										
43 *Fdd*2 *dd*2_1	h_e0l_e: $h_e + l_e = 4n + 2$ d_2	*A*	$0k_el_e$: $k_e + l_e = 4n + 2$ d_1	*A*	$0k_el_e$: $k_e + l_e = 4n + 2$ d_1 h_e0l_e: $h_e + l_e = 4n + 2$ d_2	*A*	$0k_el_e$: $k_e + l_e = 4n + 2$ d_1	A_h	h_e0l_e: $h_e + l_e = 4n + 2$ d_2	A_h
44 *Imm*2 *nn*2_1										
45 *Iba*2 *cc*2_1	h_o0l_o *a*	*A*	$0k_ol_o$ *b*	*A*	$0k_ol_o$ *b* h_o0l_o *a*	*A*	$0k_ol_o$ *b*	A_h	h_o0l_o *a*	A_h
46 *Ima*2 *nc*2_1	h_o0l_o *a*	*A*			h_o0l_o *a*	*A*			h_o0l_o *a*	A_h

Point group *mmm*

Space group	Incident-beam direction											
	[100]		[010]		[001]		[*uv*0]		[0*vw*]		[*u*0*w*]	
47 *P*2/*m*2/*m*2/*m*												
48 *P*2/*n*2/*n*2/*n*	$h0l$: $h + l =$ $2n + 1$ n_2 $hk0$: $h + k =$ $2n + 1$ n_3	*A*	$0kl$: $k + l =$ $2n + 1$ n_1 $hk0$: $h + k =$ $2n + 1$ n_3	*A*	$0kl$: $k + l =$ $2n + 1$ n_1 $h0l$: $h + l =$ $2n + 1$ n_2	*A*	$hk0$: $h + k =$ $2n + 1$ n_3	A_h	$0kl$: $k + l =$ $2n + 1$ n_1	A_h	$h0l$: $h + l =$ $2n + 1$ n_2	A_h
49 *P*2/*c*2/*c*2/*m*	$h0l_o$ c_2	*A*	$0kl_o$ c_1	*A*	$0kl_o$ c_1 $h0l_o$ c_2	*A*			$0kl_o$ c_1	A_h	$h0l_o$ c_2	A_h
50 *P*2/*b*2/*a*2/*n*	h_o0l *a* $hk0$: $h + k =$ $2n + 1$ *n*	*A*	$0k_ol$ *b* $hk0$: $h + k =$ $2n + 1$ *n*	*A*	$0k_ol$ *b* h_o0l *a*	*A*	$hk0$: $h + k =$ $2n + 1$ *n*	A_h	$0k_ol$ *b*	A_h	h_o0l *a*	A_h
51 *P*2_1/*m*2/*m*2/*a*	h_ok0 *a*	*A*	h_ok0 *a*	*A*			h_ok0 *a*	A_h				
52 *P*2/*n*2_1/*n*2/*a*	$h0l$: $h + l =$ $2n + 1$ n_2 h_ok0 *a*	*A*	$0kl$: $k + l =$ $2n + 1$ n_1 h_ok0 *a*	*A*	$0kl$: $k + l =$ $2n + 1$ n_1 $h0l$: $h + l =$ $2n + 1$ n_2	*A*	h_ok0 *a*	A_h	$0kl$: $k + l =$ $2n + 1$ n_1	A_h	$h0l$: $h + l =$ $2n + 1$ n_2	A_h
53 *P*2/*m*2/*n*2_1/*a*	$h0l$: $h + l =$ $2n + 1$ *n* h_ok0 *a*	*A*	h_ok0 *a*	*A*	$h0l$: $h + l =$ $2n + 1$ *n*	*A*	h_ok0 *a*	A_h			$h0l$: $h + l =$ $2n + 1$ *n*	A_h
54 *P*2_1/*c*2/*c*2/*a*	$h0l_o$ c_2 h_ok0 *a*	*A*	$0kl_o$ c_1 h_ok0 *a*	*A*	$0kl_o$ c_1 $h0l_o$ c_2	*A*	h_ok0 *a*	A_h	$0kl_o$ c_1	A_h	$h0l_o$ c_2	A_h

Table 2.5.3.12 (*cont.*)

Space group		Incident-beam direction											
		[100]		[010]		[001]		[*uv*0]		[0*vw*]		[*u*0*w*]	
55	$P2_1/b2_1/a2/m$	h_o0l a	A	$0k_ol$ b	A	$0k_ol$ b h_o0l a	A			$0k_ol$ b	A_h	h_o0l a	A_h
56	$P2_1/c2_1/c2/n$	$h0l_o$ c_2 $hk0$: $h + k =$ $2n + 1$ n	A	$0kl_o$ c_1 $hk0$: $h + k =$ $2n + 1$ n	A	$0kl_o$ c_1 $h0l_o$ c_2	A	$hk0$: $h + k =$ $2n + 1$ n	A_h	$0kl_o$ c_1	A_h	$h0l_o$ c_2	A_h
57	$P2/b2_1/c2_1/m$	$h0l_o$ c	A	$0k_ol$ b	A	$0k_ol$ b $h0l_o$ c	A			$0k_ol$ b	A_h	$h0l_o$ c	A_h
58	$P2_1/n2_1/n2/m$	$h0l$: $h + l =$ $2n + 1$ n_2	A	$0kl$: $k + l =$ $2n + 1$ n_1	A	$0kl$: $k + l =$ $2n + 1$ n_1 $h0l$: $h + l =$ $2n + 1$ n_2	A			$0kl$: $k + l =$ $2n + 1$ n_1	A_h	$h0l$: $h + l =$ $2n + 1$ n_2	A_h
59	$P2_1/m2_1/m2/n$	$hk0$: $h + k =$ $2n + 1$ n	A	$hk0$: $h + k =$ $2n + 1$ n	A			$hk0$: $h + k =$ $2n + 1$ n	A_h				
60	$P2_1/b2/c2_1/n$	$h0l_o$ c $hk0$: $h + k =$ $2n + 1$ n	A	$0k_ol$ b $hk0$: $h + k =$ $2n + 1$ n	A	$0k_ol$ b $h0l_o$ c	A	$hk0$: $h + k =$ $2n + 1$ n	A_h	$0k_ol$ b	A_h	$h0l_o$ c	A_h
61	$P2_1/b2_1/c2_1/a$	$h0l_o$ c h_ok0 a	A	$0k_ol$ b h_ok0 a	A	$0k_ol$ b $h0l_o$ c	A	h_ok0 a	A_h	$0k_ol$ b	A_h	$h0l_o$ c	A_h
62	$P2_1/n2_1/m2_1/a$	h_ok0 a	A	$0kl$: $k + l =$ $2n + 1$ n h_ok0 a	A	$0kl$: $k + l =$ $2n + 1$ n	A	h_ok0 a	A_h	$0kl$: $k + l =$ $2n + 1$ n	A_h		
63	$C2/m2/c2_1/m$	h_e0l_o c	A			h_e0l_o c	A					h_e0l_o c	A_h
64	$C2/m2/c2_1/a$	h_e0l_o c h_ok_o0 a	A	h_ok_o0 a	A	h_e0l_o c	A	h_ok_o0 a	A_h			h_e0l_o c	A_h
65	$C2/m2/m2/m$												
66	$C2/c2/c2/m$	h_e0l_o c_2	A	$0k_el_o$ c_1	A	$0k_el_o$ c_1 h_e0l_o c_2	A			$0k_el_o$ c_1	A_h	h_e0l_o c_2	A_h
67	$C2/m2/m2/a$	h_ok_o0 a	A	h_ok_o0 a	A			h_ok_o0 a	A_h				
68	$C2/c2/c2/a$	h_e0l_o c_2 h_ok_o0 a	A	$0k_el_o$ c_1 h_ok_o0 a	A	$0k_el_o$ c_1 h_e0l_o c_2	A	h_ok_o0 a	A_h	$0k_el_o$ c_1	A_h	h_e0l_o c_2	A_h
69	$F2/m2/m2/m$												
70	$F2/d2/d2/d$	h_e0l_e: $h_e + l_e =$ $4n + 2$ d_2 h_ek_e0: $h_e + k_e =$ $4n + 2$ d_3	A	h_ek_e0: $h_e + k_e =$ $4n + 2$ d_3 $0k_el_e$: $k_e + l_e =$ $4n + 2$ d_1	A	$0k_el_e$: $k_e + l_e =$ $4n + 2$ d_1 h_e0l_e: $h_e + l_e =$ $4n + 2$ d_2	A	h_ek_e0: $h_e + k_e =$ $4n + 2$ d_3	A_h	$0k_el_e$: $k_e + l_e =$ $4n + 2$ d_1	A_h	h_e0l_e: $h_e + l_e =$ $4n + 2$ d_2	A_h
71	$I2/m2/m2/m$												

Table 2.5.3.12 (*cont.*)

Space group	Incident-beam direction											
	[100]		[010]		[001]		[*uv*0]		[0*vw*]		[*u*0*w*]	
72 *I*2/*b*2/*a*2/*m*	h_o0l_o *a*	*A*	$0k_ol_o$ *b*	*A*	$0k_ol_o$ *b* h_o0l_o *a*	*A*			$0k_ol_o$ *b*	A_h	h_o0l_o *a*	A_h
73 $I2_1/b2_1/c2_1/a$	h_o0l_o *c* h_ok_o0 *a*	*A*	h_ok_o0 *a* $0k_ol_o$ *b*	*A*	$0k_ol_o$ *b* h_o0l_o *c*	*A*	h_ok_o0 *a*	A_h	$0k_ol_o$ *b*	A_h	h_o0l_o *c*	A_h
74 $I2_1/m2_1/m2_1/a$	h_ok_o0 *a*	*A*	h_ok_o0 *a*	*A*			h_ok_o0 *a*	A_h				

Point group 4/*m*

Space group	Incident-beam direction			
	[100], [110]		[*uv*0]	
83 *P*4/*m*				
84 $P4_2/m$				
85 *P*4/*n*	*hk*0: $h + k = 2n + 1$ *n*	*A*	*hk*0: $h + k = 2n + 1$ *n*	A_h
86 $P4_2/n$	*hk*0: $h + k = 2n + 1$ *n*	*A*	*hk*0: $h + k = 2n + 1$ *n*	A_h
87 *I*4/*m*				
88 $I4_1/a$	h_ok_o0 *a*	*A*	h_ok_o0 *a*	A_h

Point group 4*mm*. The symbol *a* in the column [*u*0*w*] is equivalent to the symbol *b* in the space groups of the first column.

Space group	Incident-beam direction									
	[100]		[001]		[110]		[*u*0*w*]		[*uuw*]	
99 *P*4*mm*										
100 *P*4*bm*	h_o0l a_2	*A*	$0k_ol$ b_1 h_o0l a_2	*A*			h_o0l *a*	A_h		
101 $P4_2cm$	$h0l_o$ c_2	*A*	$0kl_o$ c_1 $h0l_o$ c_2	*A*			$h0l_o$ *c*	A_h		
102 $P4_2nm$	*h*0*l*: $h + l = 2n + 1$ n_2	*A*	0*kl*: $k + l = 2n + 1$ n_1 *h*0*l*: $h + l = 2n + 1$ n_2	*A*			*h*0*l*: $h + l = 2n + 1$ *n*	A_h		
103 *P*4*cc*	$h0l_o$ c_{12}	*A*	$0kl_o$ c_{11} $h0l_o$ c_{12} $hhl_o, \bar{h}hl_o$ c_2	*A*	hhl_o c_2	*A*	$h0l_o$ c_1	A_h	hhl_o c_2	A_h
104 *P*4*nc*	*h*0*l*: $h + l = 2n + 1$ n_2	*A*	0*kl*: $k + l = 2n + 1$ n_1 *h*0*l*: $h + l = 2n + 1$ n_2 $hhl_o, \bar{h}hl_o$ *c*	*A*	hhl_o *c*	*A*	*h*0*l*: $h + l = 2n + 1$ *n*	A_h	hhl_o *c*	A_h
105 $P4_2mc$			$hhl_o, \bar{h}hl_o$ *c*	*A*	hhl_o *c*	*A*			hhl_o *c*	A_h
106 $P4_2bc$	h_o0l a_2	*A*	$0k_ol$ b_1 h_o0l a_2 $hhl_o, \bar{h}hl_o$ *c*	*A*	hhl_o *c*	*A*	h_o0l *a*	A_h	hhl_o *c*	A_h
107 *I*4*mm*										

Table 2.5.3.12 (*cont.*)

Space group		Incident-beam direction [100]		[001]		[110]		[$u0w$]		[uuw]	
108	$I4cm$	h_o0l_o c_2	A	$0k_ol_o$ c_1 h_o0l_o c_2	A			h_o0l_o c	A_h		
109	$I4_1md$			$hhl_e, \bar{h}hl_e$: $2h + l_e = 4n + 2$ d	A	hhl_e: $2h + l_e = 4n + 2$ d	A			hhl_e: $2h + l_e = 4n + 2$ d	A_h
110	$I4_1cd$	h_o0l_o c_2	A	$0k_ol_o$ c_1 h_o0l_o c_2 $hhl_e, \bar{h}hl_e$: $2h + l_e = 4n + 2$ d	A	hhl_e: $2h + l_e = 4n + 2$ d	A	h_o0l_o c	A_h	hhl_e: $2h + l_e = 4n + 2$ d	A_h

Point group $\bar{4}2m$. The symbol a in the column [$u0w$] is equivalent to the symbol b in the space groups of the first column.

Space group		Incident-beam direction [100]		[001]		[110]		[$u0w$]		[uuw]	
111	$P\bar{4}2m$										
112	$P\bar{4}2c$			$hhl_o, \bar{h}hl_o$ c	A	hhl_o c	A			hhl_o c	A_h
113	$P\bar{4}2_1m$										
114	$P\bar{4}2_1c$			$hhl_o, \bar{h}hl_o$ c	A	hhl_o c	A			hhl_o c	A_h
115	$P\bar{4}m2$										
116	$P\bar{4}c2$	$h0l_o$ c_2	A	$0kl_o$ c_1 $h0l_o$ c_2	A			$h0l_o$ c	A_h		
117	$P\bar{4}b2$	h_o0l a_2	A	$0k_ol$ b_1 h_o0l a_2	A			h_o0l a	A_h		
118	$P\bar{4}n2$	$h0l$: $h + l = 2n + 1$ n_2	A	$0kl$: $k + l = 2n + 1$ n_1 $h0l$: $h + l = 2n + 1$ n_2	A			$h0l$: $h + l = 2n + 1$ n	A_h		
119	$I\bar{4}m2$										
120	$I\bar{4}c2$	h_o0l_o c_2	A	$0k_ol_o$ c_1 h_o0l_o c_2	A			h_o0l_o c	A_h		
121	$I\bar{4}2m$										
122	$I\bar{4}2d$			$hhl_e, \bar{h}hl_e$: $2h + l_e = 4n + 2$ d	A	hhl_e: $2h + l_e = 4n + 2$ d	A			hhl_e: $2h + l_e = 4n + 2$ d	A_h

Point group $4/mmm$. The symbol a in the column [$u0w$] is equivalent to the symbol b in the space groups of the first column.

Space group		Incident-beam direction [100]		[001]		[110]		[$u0w$]		[uuw]		[$uv0$]	
123	$P4/mmm$ $P4/m2/m2/m$												
124	$P4/mcc$ $P4/m2/c2/c$	$h0l_o$ c_{12}	A	$0kl_o$ c_{11} $h0l_o$ c_{12} $hhl_o, \bar{h}hl_o$ c_2	A	hhl_o c_2	A	$h0l_o$ c_1	A_h	hhl_o c_2	A_h		
125	$P4/nbm$ $P4/n2/b2/m$	$hk0$: $h + k =$ $2n + 1$ n h_o0l a_2	A	$0k_ol$ b_1 h_o0l a_2	A	$hk0$: $h + k =$ $2n + 1$ n	A	h_o0l a	A_h			$hk0$: $h + k =$ $2n + 1$ n	A_h

Table 2.5.3.12 (*cont.*)

Space group		Incident-beam direction											
		[100]		[001]		[110]		[$u0w$]		[uuw]		[$uv0$]	
126	$P4/nnc$ $P4/n2/n2/c$	$hk0$: $h+k=$ $2n+1$ n_1 $h0l$: $h+l=$ $2n+1$ n_{22}	A	$0kl$: $k+l=$ $2n+1$ n_{21} $h0l$: $h+l=$ $2n+1$ n_{22} $hhl_o, \bar{h}hl_o$ c	A	$hk0$: $h+k=$ $2n+1$ n_1 hhl_o c	A	$h0l$: $h+l=$ $2n+1$ n_2	A_h	hhl_o c	A_h	$hk0$: $h+k=$ $2n+1$ n_1	A_h
127	$P4/mbm$ $P4/m2_1/b2/m$	h_o0l a_2	A	$0k_ol$ b_1 h_o0l a_2	A			h_o0l a	A_h				
128	$P4/mnc$ $P4/m2_1/n2/c$	$h0l$: $h+l=$ $2n+1$ n_2	A	$0kl$: $k+l=$ $2n+1$ n_1 $h0l$: $h+l=$ $2n+1$ n_2 $hhl_o, \bar{h}hl_o$ c	A	hhl_o c	A	$h0l$: $h+l=$ $2n+1$ n	A_h	hhl_o c	A_h		
129	$P4/nmm$ $P4/n2_1/m2/m$	$hk0$: $h+k=$ $2n+1$ n	A			$hk0$: $h+k=$ $2n+1$ n	A					$hk0$: $h+k=$ $2n+1$ n	A_h
130	$P4/ncc$ $P4/n2_1/c2/c$	$hk0$: $h+k=$ $2n+1$ n $h0l_o$ c_{12}	A	$0kl_o$ c_{11} $h0l_o$ c_{12} $hhl_o, \bar{h}hl_o$ c_2	A	$hk0$: $h+k=$ $2n+1$ n hhl_o c_2	A	$h0l_o$ c_1	A_h	hhl_o c_2	A_h	$hk0$: $h+k=$ $2n+1$ n	A_h
131	$P4_2/mmc$ $P4_2/m2/m2/c$			$hhl_o, \bar{h}hl_o$ c	A	hhl_o c	A			hhl_o c	A_h		
132	$P4_2/mcm$ $P4_2/m2/c2/m$	$h0l_o$ c_2	A	$0kl_o$ c_1 $h0l_o$ c_2	A			$h0l_o$ c	A_h				
133	$P4_2/nbc$ $P4_2/n2/b2/c$	$hk0$: $h+k=$ $2n+1$ n h_o0l a_2	A	$0k_ol$ b_1 h_o0l a_2 $hhl_o, \bar{h}hl_o$ c	A	$hk0$: $h+k=$ $2n+1$ n hhl_o c	A	h_o0l a	A_h	hhl_o c	A_h	$hk0$: $h+k=$ $2n+1$ n	A_h
134	$P4_2/nnm$ $P4_2/n2/n2/m$	$hk0$: $h+k=$ $2n+1$ n_1 $h0l$: $h+l=$ $2n+1$ n_{22}	A	$0kl$: $k+l=$ $2n+1$ n_{21} $h0l$: $h+l=$ $2n+1$ n_{22}	A	$hk0$: $h+k=$ $2n+1$ n_1	A	$h0l$: $h+l=$ $2n+1$ n_2	A_h			$hk0$: $h+k=$ $2n+1$ n_1	A_h
135	$P4_2/mbc$ $P4_2/m2_1/b2/c$	h_o0l a_2	A	$0k_ol$ b_1 h_o0l a_2 $hhl_o, \bar{h}hl_o$ c	A	hhl_o c	A	h_o0l a	A_h	hhl_o c	A_h		
136	$P4_2/mnm$ $P4_2/m2_1/n2/m$	$h0l$: $h+l=$ $2n+1$ n_2	A	$0kl$: $k+l=$ $2n+1$ n_1 $h0l$: $h+l=$ $2n+1$ n_2	A			$h0l$: $h+l=$ $2n+1$ n	A_h				

Table 2.5.3.12 (*cont.*)

Space group		Incident-beam direction											
		[100]		[001]		[110]		[$u0w$]		[uuw]		[$uv0$]	
137	$P4_2/nmc$ $P4_2/n2_1/m2/c$	$hk0$: $h+k=$ $2n+1$ n	A	hhl_o, $\bar{h}hl_o$ c	A	hhl_o c $hk0$: $h+k=$ $2n+1$ n	A			hhl_o c	A_h	$hk0$: $h+k=$ $2n+1$ n	A_h
138	$P4_2/ncm$ $P4_2/n2_1/c2/m$	$hk0$: $h+k=$ $2n+1$ n $h0l_o$ c_2	A	$0kl_o$ c_1 $h0l_o$ c_2	A	$hk0$: $h+k=$ $2n+1$ n	A	$h0l_o$ c	A_h			$hk0$: $h+k=$ $2n+1$ n	A_h
139	$I4/mmm$ $I4/m2/m2/m$												
140	$I4/mcm$ $I4/m2/c2/m$	h_o0l_o c_2	A	$0k_ol_o$ c_1 h_o0l_o c_2	A			h_o0l_o c	A_h				
141	$I4_1/amd$ $I4_1/a2/m2/d$	h_ok_o0 a	A	hhl_e, $\bar{h}hl_e$: $2h+l_e=$ $4n+2$ d	A	h_ok_o0 a hhl_e: $2h+l_e=$ $4n+2$ d	A			hhl_e: $2h+l_e=$ $4n+2$ d	A_h	h_ok_o0 a	A_h
142	$I4_1/acd$ $I4_1/a2/c2/d$	h_ok_o0 a h_o0l_o c_2	A	$0k_ol_o$ c_1 h_o0l_o c_2 hhl_e, $\bar{h}hl_e$: $2h+l_e=$ $4n+2$ d	A	h_ok_o0 a hhl_e: $2h+l_e=$ $4n+2$ d	A	h_o0l_o c	A_h	hhl_e: $2h+l_e=$ $4n+2$ d	A_h	h_ok_o0 a	A_h

Point groups $3m$, $\bar{3}m$

Space group		Incident-beam direction									
		[0001]		[$11\bar{2}0$]		[$1\bar{1}00$]		[$11\bar{2}w$]		[$1\bar{1}0w$]	
156	$P3m1$										
157	$P31m$										
158	$P3c1$	$h\bar{h}0l_o$, $0h\bar{h}l_o$, $\bar{h}0hl_o$ c	A			$h\bar{h}0l_o$ c	A			$h\bar{h}0l_o$ c	A_h
159	$P31c$	$hh\overline{2h}l_o$, $h\overline{2h}hl_o$, $\overline{2h}hhl_o$ c	A	$hh\overline{2h}l_o$ c	A			$hh\overline{2h}l_o$ c	A_h		
160	$R3m$										
161	$R3c$	$h\bar{h}0l_o$, $0h\bar{h}l_o$, $\bar{h}0hl_o$: $h+l_o=3n$ c	A_h			$h\bar{h}0l_o$: $h+l_o=3n$ c	A_h			$h\bar{h}0l_o$: $h+l_o=3n$ c	A_h
162	$P\bar{3}1m$										
163	$P\bar{3}1c$	$hh\overline{2h}l_o$, $h\overline{2h}hl_o$, $\overline{2h}hhl_o$ c	A	$hh\overline{2h}l_o$ c	A			$hh\overline{2h}l_o$ c	A_h		
164	$P\bar{3}m1$										
165	$P\bar{3}c1$	$h\bar{h}0l_o$, $0h\bar{h}l_o$, $\bar{h}0hl_o$ c	A			$h\bar{h}0l_o$ c	A			$h\bar{h}0l_o$ c	A_h
166	$R\bar{3}m$										
167	$R\bar{3}c$	$h\bar{h}0l_o$, $0h\bar{h}l_o$, $\bar{h}0hl_o$: $h+l_o=3n$ c	A_h			$h\bar{h}0l_o$: $h+l_o=3n$ c	A_h			$h\bar{h}0l_o$: $h+l_o=3n$ c	A_h

Point groups $6mm$, $\bar{6}m2$, $6/mmm$

Space group		Incident-beam direction									
		[0001]		[$11\bar{2}0$]		[$1\bar{1}00$]		[$11\bar{2}w$]		[$1\bar{1}0w$]	
183	$P6mm$										
184	$P6cc$	$h\bar{h}0l_o$, $0h\bar{h}l_o$, $\bar{h}0hl_o$ c_1 $hh\overline{2h}l_o$, $h\overline{2h}hl_o$, $\overline{2h}hhl_o$ c_2	A	$hh\overline{2h}l_o$ c_2	A	$h\bar{h}0l_o$ c_1	A	$hh\overline{2h}l_o$ c_2	A_h	$h\bar{h}0l_o$ c_1	A_h

Table 2.5.3.12 (*cont.*)

Space group		Incident-beam direction [0001]		[11$\bar{2}$0]		[1$\bar{1}$00]		[11$\bar{2}$*w*]		[1$\bar{1}$0*w*]	
185	$P6_3cm$	$h\bar{h}0l_o, 0h\bar{h}l_o, \bar{h}0hl_o$ c	A			$h\bar{h}0l_o$ c	A			$h\bar{h}0l_o$ c	A_h
186	$P6_3mc$	$hh\overline{2h}l_o, h\overline{2h}hl_o, \overline{2h}hhl_o$ c	A	$hh\overline{2h}l_o$ c	A			$hh\overline{2h}l_o$ c	A_h		
187	$P\bar{6}m2$										
188	$P\bar{6}c2$	$h\bar{h}0l_o, 0h\bar{h}l_o, \bar{h}0hl_o$ c	A			$h\bar{h}0l_o$ c	A			$h\bar{h}0l_o$ c	A_h
189	$P\bar{6}2m$										
190	$P\bar{6}2c$	$hh\overline{2h}l_o, h\overline{2h}hl_o, \overline{2h}hhl_o$ c	A	$hh\overline{2h}l_o$ c	A			$hh\overline{2h}l_o$ c	A_h		
191	$P6/mmm$										
192	$P6/mcc$	$h\bar{h}0l_o, 0h\bar{h}l_o, \bar{h}0hl_o$ c_1 $hh\overline{2h}l_o, h\overline{2h}hl_o, \overline{2h}hhl_o$ c_2	A	$hh\overline{2h}l_o$ c_2	A	$h\bar{h}0l_o$ c_1	A	$hh\overline{2h}l_o$ c_2	A_h	$h\bar{h}0l_o$ c_1	A_h
193	$P6_3/mcm$	$h\bar{h}0l_o, 0h\bar{h}l_o, \bar{h}0hl_o$ c	A			$h\bar{h}0l_o$ c	A			$h\bar{h}0l_o$ c	A_h
194	$P6_3/mmc$	$hh\overline{2h}l_o, h\overline{2h}hl_o, \overline{2h}hhl_o$ c	A	$hh\overline{2h}l_o$ c	A			$hh\overline{2h}l_o$ c	A_h		

Point group $m3$

Space group		Incident-beam direction [100]		[110]		[*uv*0]	
200	$Pm3$ $P2/m\bar{3}$						
201	$Pn3$ $P2/n\bar{3}$	$h0l$: $h + l = 2n + 1$ n_2 $hk0$: $h + k = 2n + 1$ n_3	A	$hk0$: $h + k = 2n + 1$ n_3	A	$hk0$: $h + k = 2n + 1$ n	A_h
202	$Fm3$ $F2/m\bar{3}$						
203	$Fd3$ $F2/d\bar{3}$	h_e0l_e: $h_e + l_e = 4n + 2$ d_2 h_ek_e0: $h_e + k_e = 4n + 2$ d_3	A	h_ek_e0: $h_e + k_e = 4n + 2$ d_3	A	h_ek_e0: $h_e + k_e = 4n + 2$ d	A_h
204	$Im3$ $I2/m\bar{3}$						
205	$Pa3$ $P2_1/a\bar{3}$	$h0l_o$ c_2 h_ok0 a_3	A	h_ok0 a_3	A^*	h_ok0 a	A_h
206	$Ia3$ $I2_1/a\bar{3}$	h_o0l_o c_2 h_ok_o0 a_3	A	h_ok_o0 a_3	A	h_ok_o0 a	A_h

Point group $\bar{4}3m$. The symbol a in the column [100] is equivalent to the symbol c in the space groups of the first column.

Space group		Incident-beam direction [100]		[110]		[*uuw*]	
215	$P\bar{4}3m$						
216	$F\bar{4}3m$						
217	$I\bar{4}3m$						
218	$P\bar{4}3n$	$h_okk, h_ok\bar{k}$ n	A	hhl_o n	A	hhl_o n	A_h
219	$F\bar{4}3c$	$h_ok_ok_o, h_ok_o\bar{k}_o$ a	A	$h_oh_ol_o$ c	A	$h_oh_ol_o$ c	A_h
220	$I\bar{4}3d$	$h_ekk, h_ek\bar{k}$: $2k + h_e = 4n + 2$ d	A	hhl_e: $2h + l_e = 4n + 2$ d	A	hhl_e: $2h + l_e = 4n + 2$ d	A_h

Table 2.5.3.12 (*cont.*)

Point group $m3m$. The symbol a in the column [100] is equivalent to the symbol c in the space groups of the first column.

Space group		Incident-beam direction							
		[100]		[110]		[$uv0$]		[uuw]	
221	$Pm3m$ $P4/m\bar{3}2/m$								
222	$Pn3n$ $P4/n\bar{3}2/n$	$h0l$: $h+l=2n+1$ n_{12} $hk0$: $h+k=2n+1$ n_{13} h_okk, $h_o\bar{k}k$ n_2	A	$hk0$: $h+k=2n+1$ n_{13} hhl_o n_2	A	$hk0$: $h+k=2n+1$ n_1	A_h	hhl_o n_2	A_h
223	$Pm3n$ $P4_2/m\bar{3}2/n$	h_okk, $h_o\bar{k}k$ n	A	hhl_o n	A			hhl_o n	A_h
224	$Pn3m$ $P4_2/n\bar{3}2/m$	$h0l$: $h+l=2n+1$ n_2 $hk0$: $h+k=2n+1$ n_3	A	$hk0$: $h+k=2n+1$ n_3	A	$hk0$: $h+k=2n+1$ n	A_h		
225	$Fm3m$ $F4/m\bar{3}2/m$								
226	$Fm3c$ $F4/m\bar{3}2/c$	$h_ok_ok_o$, $h_o\bar{k}_ok_o$ a	A	$h_oh_ol_o$ c	A			$h_oh_ol_o$ c	A_h
227	$Fd3m$ $F4_1/d\bar{3}2/m$	h_e0l_e: $h_e+l_e=4n+2$ d_2 h_ek_e0: $h_e+k_e=4n+2$ d_3	A	h_ek_e0: $h_e+k_e=4n+2$ d_3	A	h_ek_e0: $h_e+k_e=4n+2$ d	A_h		
228	$Fd3c$ $F4_1/d\bar{3}2/c$	h_e0l_e: $h_e+l_e=4n+2$ d_2 h_ek_e0: $h_e+k_e=4n+2$ d_3 $h_ok_ok_o$, $h_o\bar{k}_ok_o$ a	A	$h_oh_ol_o$ c h_ek_e0: $h_e+k_e=4n+2$ d_3	A	h_ek_e0: $h_e+k_e=4n+2$ d	A_h	$h_oh_ol_o$ c	A_h
229	$Im3m$ $I4/m\bar{3}2/m$								
230	$Ia3d$ $I4_1/a\bar{3}2/d$	h_ok_o0 a_3 h_o0l_o c_2 h_ekk, $h_e\bar{k}k$: $2k+h_e=4n+2$ d	A	hhl_e: $2h+l_e=4n+2$ d h_ok_o0 a_3	A	h_ok_o0 a	A_h	hhl_e: $2h+l_e=4n+2$ d	A_h

are no kinematically forbidden reflections. Thus, the lattice type is determined to be primitive P.

Possible space groups which satisfy point group $4/mmm$ and primitive lattice type P are those of Nos. 123–138 in Table 2.5.3.9. In Fig. 2.5.3.15(a), the dynamical extinction line A_2 is seen in the 100 disc and in the equivalent 010 disc. By consulting Table 2.5.3.9, four space groups $P4/mbm$, $P4/mnc$, $P4_2/mbc$ and $P4_2/mnm$ are selected. In Fig. 2.5.3.15(b), the dynamical extinction line A_2 is seen in the 010 disc but not in the $10\bar{1}$ disc. Two space groups $P4/mnc$ and $P4_2/mnm$ are selected from the four. To distinguish the two space groups, it is found from Table 2.5.3.9 that a CBED pattern taken with the [110] electron incidence should be examined. Fig. 2.5.3.15(e) shows a CBED pattern taken with the [110] incidence at 100 kV, where the 001 reflection is exactly excited. The $h\bar{h}1$ reflections are kinematically allowed for space group $P4_2/mnm$ but kinematically forbidden for $P4/mnc$. Since in the case of $P4/mnc$, no *Umweganregung* (multiple scattering) paths to the 001 reflection exist in the zeroth-order Laue zone, only the intensities of HOLZ lines, which are caused by *Umweganregung via* HOLZ reflections, are expected to appear in the 001 disc. If such *Umweganregung* is not practically excited, the 001 reflection must have no intensity. However, strong intensity produced by two-dimensional interaction is seen in the 001 disc of Fig. 2.5.3.15(e). This indicates that the reflection is an allowed reflection. Therefore, the space group of rutile is determined to be $P4_2/mnm$, which agrees with the space group already known.

Samarium selenide (Sm_3Se_4). Sm_3Se_4 has the Th_3P_4 structure type with space group $I\bar{4}3d$ at high temperatures. The lattice parameters are $a = b = c = 0.8885$ nm. It was expected that Sm_3Se_4 would transform to an ordered state of electrons with two valences of +2 and +3 around 150 K. The determination of the space group of the material was conducted at 100 K and room temperature. The space groups at both temperatures were determined by CBED to be the same. The following experiments were performed at 100 K.

Fig. 2.5.3.16(a) shows a CBED pattern taken with the [111] incidence at 80 kV, which clearly shows the first-order-Laue-zone reflections. The symmetry of the WP is seen to be $3m$ with the help of the enlarged insets. Possible diffraction groups are $3m$, $3m1_R$ and 6_Rmm_R from Table 2.5.3.3. Fig. 2.5.3.16(b), which is the central part of Fig. 2.5.3.16(a), shows projection symmetry $3m$, indicating that the projection diffraction group is $3m1_R$. Among the three groups $3m$, $3m1_R$ and 6_Rmm_R, diffraction groups for which the projection diffraction group is $3m1_R$ are $3m$ and $3m1_R$. Possible point groups are found to be $3m$, $\bar{4}3m$ and $\bar{6}m2$ from Fig. 2.5.3.4. Fig. 2.5.3.16(c) shows a CBED pattern taken with the [100] incidence at 80 kV. The WP is seen to have symmetry $2mm$. Allowed diffraction groups are $2mm$, $2mm1_R$ and 4_Rmm_R. Fig. 2.5.3.16(d), which is the central part of Fig. 2.5.3.16(c), shows projection WP symmetry $4mm$, indicating that the projection diffraction group is $4mm1_R$. The diffraction group among the three groups $2mm$, $2mm1_R$ and 4_Rmm_R whose projection diffraction group is $4mm1_R$ is 4_Rmm_R. Possible point groups are found to be $\bar{4}3m$ and $\bar{4}2m$ from Fig. 2.5.3.4. Thus, the point group

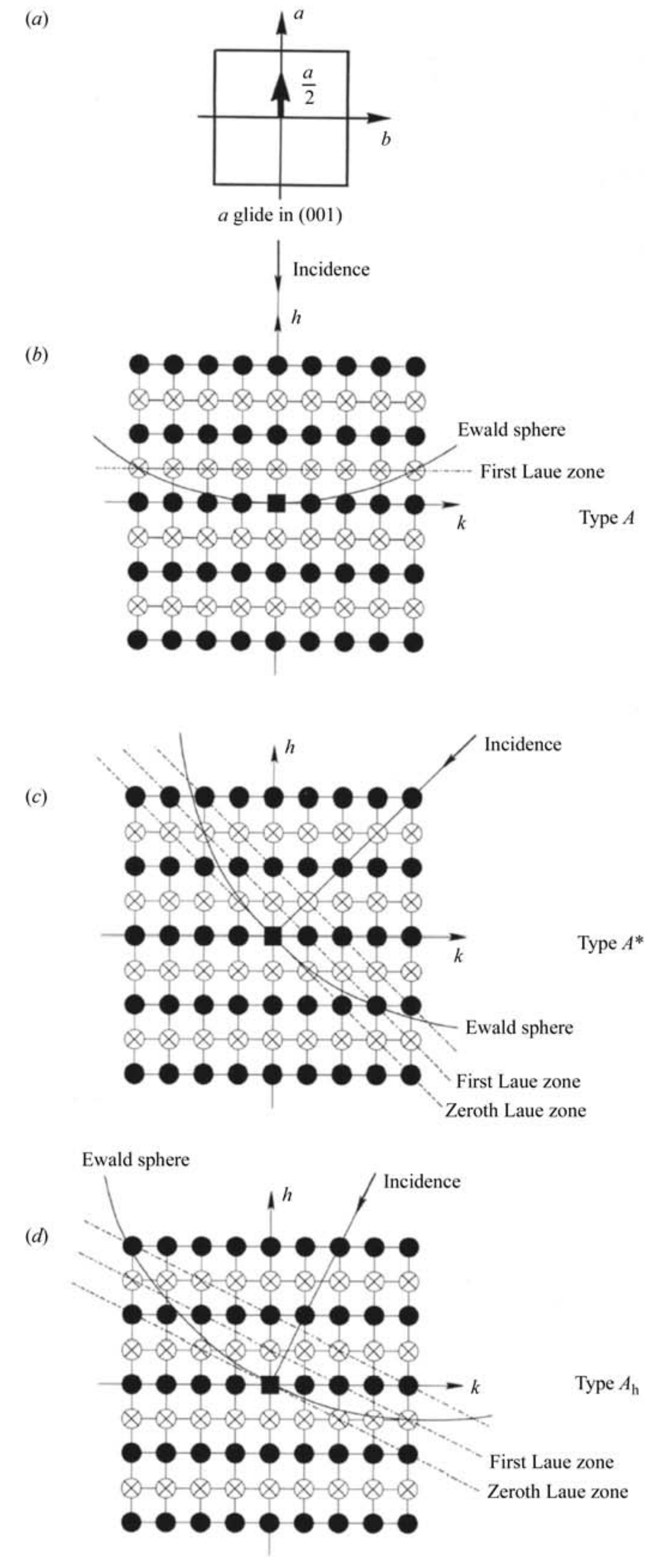

Fig. 2.5.3.13. Illustration of dynamical extinction lines appearing in HOLZ reflections due to glide planes. Black circles and circled crosses show kinematically allowed and kinematically forbidden reflections, respectively. (*a*) *a* glide in the (001) plane. (*b*) [100] incidence: dynamical extinction lines are formed in HOLZ reflections on both sides of the incident beam (type *A*). (*c*) [110] incidence: an extinction line is formed at a HOLZ reflection on one side of the incident beam because on the other side the Ewald sphere intersects an allowed HOLZ reflection (type *A**). (*d*) An incidence between [100] and [110]: an extinction line is formed at a HOLZ reflection on one side of the incident beam because on the other side the Ewald sphere does not intersect a HOLZ reflection (type A_h).

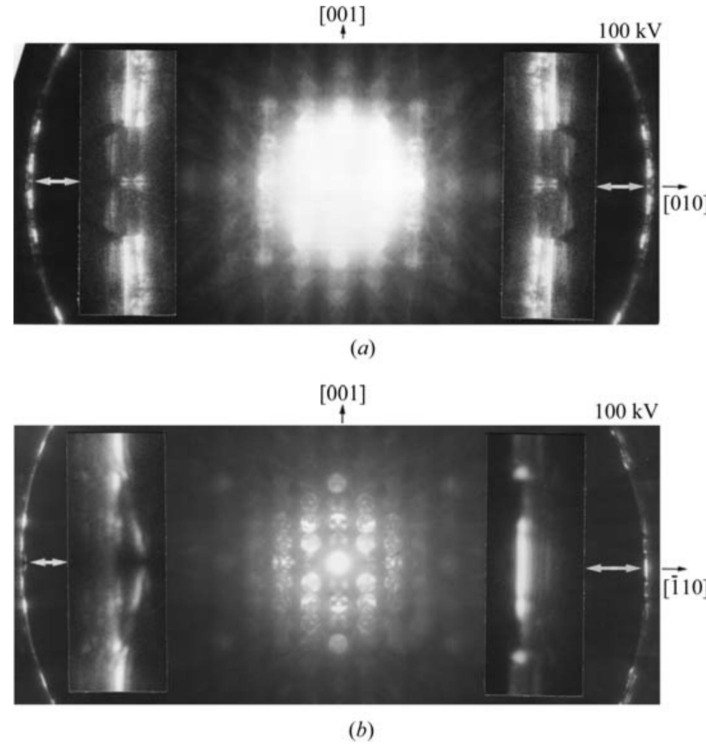

Fig. 2.5.3.14. HOLZ CBED pattern of FeS_2. (*a*) [100] incidence: type *A* dynamical extinction lines are seen clearly in the enlarged insets. (*b*) [110] incidence: a type *A** dynamical extinction line is seen clearly in the enlarged insets.

which satisfies the results obtained at the two crystal orientations is $\bar{4}3m$.

Fig. 2.5.3.16(*e*) shows an ordinary diffraction pattern taken with the [100] incidence at 80 kV. With the help of the lattice parameters and the camera length, the indices of the reflections are given as shown in the figure. The reflections $0kl$ ($k + l = 2n + 1$) are found to be kinematically forbidden. Thus, the lattice type is determined to be *I*.

The space groups having point group $\bar{4}3m$ and lattice type *I* are $I\bar{4}3m$ and $I\bar{4}3d$ from Table 2.5.3.9. Fig. 2.5.3.16(*d*) shows dynamical extinction lines A_2 in the 033 disc and equivalent discs (also broad lines A_2 in the 011 discs). Since the former space group does not give any dynamical extinction lines, the space group is determined to be $I\bar{4}3d$. For confirmation, a CBED pattern which contains the second-order-Laue-zone reflections was taken (Fig. 2.5.3.16*f*). Dynamical extinction lines *A* are seen in the 2,22,22 disc and the equivalent discs. This result also identifies the space group to be not $I\bar{4}3m$ but $I\bar{4}3d$ with the aid of Table 2.5.3.12.

2.5.3.4. *Symmetry determination of incommensurate crystals*

2.5.3.4.1. *General remarks*

Incommensurately modulated crystals do not have three-dimensional lattice periodicity. The crystals, however, recover lattice periodicity in a space higher than three dimensions. de Wolff (1974, 1977) showed that one-dimensional displacive and substitutionally modulated crystals can be described as a three-dimensional section of a (3 + 1)-dimensional periodic crystal. Janner & Janssen (1980*a*,*b*) developed a more general approach for describing a modulated crystal with *n* modulations as $(3 + n)$-dimensional periodic crystals ($n = 1, 2, \ldots$). Yamamoto (1982) derived a general structure-factor formula for *n*-dimensionally modulated crystals ($n = 1, 2, \ldots$), which holds for both displacive and substitutionally modulated crystals. Tables of the (3 + 1)-dimensional space groups for one-dimensional incommensurately modulated crystals were given by de Wolff *et al.* (1981), where the wavevector of the modulation was assumed to lie in the

references